Available online at www.sciencedirect.com
SCIENCE DIRECT®
PERGAMON
International Journal of Mechanical Sciences 45 (2003) 449–467
International Journal of MECHANICAL SCIENCES
www.elsevier.com/locate/ijmecsci

New results for the fretting-induced stress concentration on Hertzian and flat rounded contacts

M. Ciavarella[a,*], G. Macina[b]

[a] *CNR IRIS, COMES Computational Mechanics of Solids, Str. Crocefisso, 2/B, 70126 Bari, Italy*
[b] *CEMEC - Politecnico di Bari, via Amendola 126/B, 70126 Bari, Italy*

Received 31 July 2002; received in revised form 17 March 2003; accepted 24 March 2003

Abstract

Recent work on fretting fatigue has emphasized the role of stress concentration on fretting damage, while previous work had concentrated on empirical parameters to assess influence of fretting on fatigue life. In particular, analogies with fatigue in the presence of a crack or a notch have been noticed, suggesting that the stress field induced by frictional contact per se may explain the reduction of fatigue life due to fretting.

In the paper, new analytical and numerical solutions are produced for the stress concentration induced in typical fretting contacts involving the Hertzian geometry or the flat punch with rounded corners in view of application to the dovetail joints. Normal and tangential load (in the Cattaneo–Mindlin sense) is considered with "moderate" or "large" bulk stresses.

Keywords: Fretting fatigue; Stress concentration

1. Introduction

Fretting fatigue (FF) has been till recently mainly considered as an area at the boundary between fatigue, fracture and tribology. The problem is receiving increasing interest as one of the greatest cause of premature failure for gas turbine engines. One of the sites of most critical relevance for FF is generally dovetail attachment of the blade roots, the basic design of which has remained unchanged for several decades now.

When FF was first studied years ago [1,2], no detailed knowledge was available of the stress fields induced by the frictional contact (nor many concepts of fatigue and fracture mechanics were available). Therefore, the mechanical damage over the surface was considered to have a dominant

* Corresponding author. Fax: +39-080-5482533.
E-mail address: m.ciavarella@area.ba.cnr.it (M. Ciavarella).

0020-7403/03/$ - see front matter © 2003 Elsevier Science Ltd. All rights reserved.
doi:10.1016/S0020-7403(03)00061-4

role in decreasing the fatigue performance of the material. Accordingly, parameters as microslip amplitude and surface energy dissipated by friction were considered [3–5], but their efficacy, not even for the fatigue life initiation, was never proved satisfactorily.

More recently, there is an attempt to identify the aspects of FF similar to *fatigue from a stress raiser feature*. For the limiting case of square-ended punch, a simple *crack analogue* model has been suggested [6], where complete contact induces singular pressure and frictional shear tractions, motivating the use of fracture mechanics: it is recognized that, at least under these limiting conditions, initiation life is reduced to zero and the only meaningful regimes, depending on stress intensity factors amplitudes, are (i) propagation, above the threshold $\Delta K > \Delta K_{th}$, or (ii) self-arrest, for ΔK below the threshold.

For cases where we expect a smooth transition to zero pressure at the contact area edges, and correspondingly a finite stress concentration, a *notch analogue* has been proposed [7] suggesting that, at least for a contact geometry close to the singular one, the stress field induced is a perturbation of the crack analogue correspondent, as it is for a rounded crack in the Creager–Paris equations. Therefore, conditions for initiation are similar to those for a rounded crack. However, independently on the fitting the stress field with Creager–Paris equations or similar, it is simple to write down the condition of initiation as a function of the peak stress, but this does not distinguish if the crack propagates of self-arrest, and indeed it is well known that non/propagating cracks are found at the apex of notches. From a related perspective, the use of stress concentration factor alone is certainly an over/conservative assumption, asymptotically correct towards the limit of very large size of contact areas.

Solutions to frictional contact problems appropriate to fretting are obtained in closed form for the simplest cases. In the Hertzian 3D most general case under constant normal load and sequentially applied tangential load the solution has been obtained by Cattaneo [8] and the technique has been extended to the case of 2D Hertzian geometry also with " moderate" bulk by Nowell and Hills [9]. This paper will concentrate on 2D geometries such as Hertzian and rounded flat geometry, and produce new results either analytically or numerically. Although general results are valid for the Cattaneo loading condition for frictional contact of half-planes of arbitrary geometry [10,11] and in particular for the flat-rounded geometry [10], in the presence of bulk stresses, the contact problem and the stress field induced is *less* easily obtained. Given the importance of the stress concentration factor calculation under this condition representative of many fretting fatigue tests, the present paper will therefore provide new results for the contact tractions and internal stress field for various cases (the contact problem geometry is shown in Fig. 1).

In particular:

(1) *for the Hertzian geometry* previously considered by Nowell and Hills [9]:

- the case of bulk stress alone is solved in closed form, including the tensile stress concentration, whereas both were only numerically obtained previously;
- a new analytical result is obtained for the tensile stress concentration in the case of moderate bulk stress, for which a closed form solution was known only for the traction distribution;
- an improved numerical technique is given for the case of large bulk stress.

Results are documented for the tensile stress concentration over the entire range of loads.

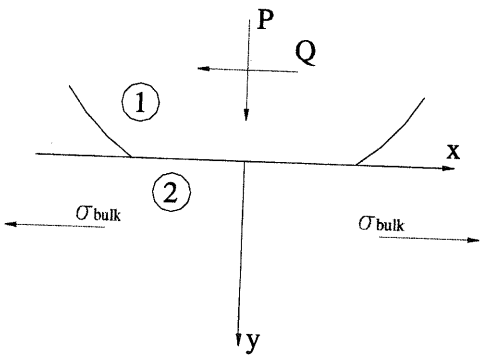

Fig. 1. Typical Hertzian fretting contact problem.

(2) *for the rounded flat (RF) geometry,*

- a closed form solution is given for the case of Cattaneo–Mindlin loading, using recent results by Jäger [13],
- an approximate close form result is obtained also for bulk stress only.
- all other cases are solved using the numerical method as in the Hertzian case with large bulk stress.

2. Hertzian contact

Within the assumption of considering the bodies elastically similar half-planes, solution for the normal load and tangential can be obtained very simply as normal and shearing tractions are uncoupled: pure normal load does not induce shearing tractions, and any kind of tangential load does not alter the pressure distribution. General solutions have been known for some time. We therefore assume that, under Hertzian cylindrical contact, with reference to Fig. 1, the two surface on contact are subjected to a pressure $p(x)$ given by

$$p(x) = -\frac{P}{\pi b}\sqrt{1-\left(\frac{x}{b}\right)^2}, \tag{1}$$

where P is the normal force per unit length and b is the contact half-width. In the following, we assume that the normal load is kept constant—a condition often followed in experiments. Also, we will compute only the stresses at maximum load, considering that extension to unloading and cyclic loading will be routine.

Therefore, we assume tangential load and bulk stresses are applied simultaneously and in phase, and the appropriate integral equation on tangential relative displacements, together with Coulomb's law for friction, give the resulting shear traction distribution.

Depending on the contact loads conditions, it is possible to quantify the tensile stress field, and particularly the surface stress, in view of its importance in fatigue life assessment. Giannakopoulos et al. [7] recently indicated an analogy with the maximum tensile stress with that of a notched

component. The tangential distribution generates tensile stresses at the trailing edge of the contact, while the normal pressure has no influence on tensile stresses for a true half-plane geometry.

Hence it is useful to quantify the maximum tensile stress σ_{xx} in the trailing edge ($x = b, y = 0$). For an half-plane problem the general expression for the surface stress in trailing edge is given by

$$\sigma_{xx}(b,0) = \frac{2}{\pi}\int_{-b}^{b} \frac{q(t)}{b-t}\,\mathrm{d}t + \sigma_b, \tag{2}$$

where $q(t)$ depends on the load case and σ_b is the bulk load. In Hills et al. [14] the Hertz case is treated in details. In particular for complete sliding case ($Q/fP = 1, \sigma_b = 0$) we have $q(x) = fp(x)$ and so

$$\sigma_{xx}(b,0) = 2fp_{max}, \tag{3}$$

where $p_{max} = 2P/\pi b$.

2.1. Bulk stress only

For the situation where the bulk tension alone is imposed and the shear load Q is equal to zero, the solving equation for the shear tractions $q(x)$ becomes [9]

$$\int_{-b}^{b} \frac{q(t)}{x-t}\,\mathrm{d}t + \frac{\pi\sigma_b}{4} = 0, \quad |x| \leqslant c, \tag{4}$$

where $2c$ is the width of the stick area and σ is the bulk load.

The presence of the bulk load alone generates a skew-symmetrical shear traction distribution. Moreover, as there is no tangential force, we can expect the stick area to be symmetrical. Accordingly, in the slip area the tangential traction is

$$q_{slip}(x) = fp_{max}\sqrt{1-(x/b)^2}\,sign(x), \quad c \leqslant |x| \leqslant b. \tag{5}$$

where p_{max} is $2P/\pi b$.

This problem, for the evident skew-symmetrical properties, was approached with a numerical technique in [9]. Here, it will be solved in closed form using Spence's technique [15]; we start by putting

$$q(x) = \begin{cases} q^*(x), & |x| \leqslant c, \\ q_{slip}(x), & c \leqslant |x| \leqslant b. \end{cases} \tag{6}$$

Eq. (4), taking into account of Eqs. (5) and (6), becomes

$$\int_{-b}^{-c} -\frac{fp_{max}\sqrt{1-(t/b)^2}}{x-t}\,\mathrm{d}t + \int_{-c}^{c} \frac{q^*(t)}{x-t}\,\mathrm{d}t + \int_{c}^{b} \frac{fp_{max}\sqrt{1-(t/b)^2}}{x-t}\,\mathrm{d}t + \frac{\sigma_b\pi}{4} = 0. \tag{7}$$

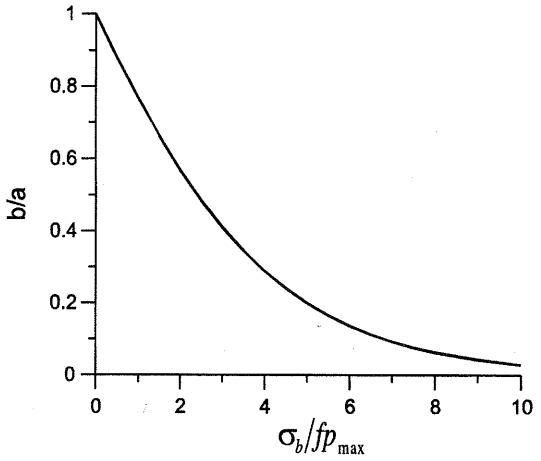

Fig. 2. Hertzian contact and bulk stress only: variation of stick zone size b/a as a function of bulk stress.

The integral in the square bracket in Eq. (15) gives

$$\int_0^c \frac{1}{(t^2-y^2)(x^2-y^2)\sqrt{c^2-y^2}}\,\mathrm{d}y = -\frac{\pi/2}{t(t^2-x^2)\sqrt{t^2-c^2}} \tag{16}$$

Hence, Eq. (14) becomes

$$q^*(x) = \frac{2}{\pi} fp_{max} x\sqrt{c^2-x^2}\int_c^b \frac{\sqrt{1-(t/b)^2}}{\sqrt{t^2-c^2}(t^2-x^2)}\,\mathrm{d}t \tag{17}$$

which can be expressed using elliptic integrals

$$q^*(x) = \frac{2}{\pi} fp_{max}\frac{x}{b}\sqrt{\frac{c^2}{b^2}-\frac{x^2}{b^2}}\left[\Pi\left(\sqrt{\frac{b^2-c^2}{b^2-x^2}},\sqrt{1-\frac{c^2}{b^2}}\right) - K\left(\sqrt{1-\frac{c^2}{b^2}}\right)\right], \tag{18}$$

where $\Pi(n,m)$ is the complete elliptic integral of the third type.

In Fig. 3 the shear tractions are plotted for different values of $\sigma_b/fp_{max}(0.5, 1.5, 3)$. Using Eq. (2) we find for the maximum stress after some algebra

$$\sigma_{xx}(b,0) = \frac{1+\sqrt{1-(c/b)^2}}{2}\sigma_b + \frac{4}{\pi} fp_{max}\sqrt{1-\left(\frac{c}{b}\right)^2}\,E\left(\sqrt{1-\left(\frac{c}{b}\right)^2}\right). \tag{19}$$

The effect of σ_b is highly non-linear and in particular we can notice that $\sigma_{xx}(b,0) \to \sigma_b + 4fp_{max}/\pi$ for large ratios σ_b/fp_{max}, when $c \to 0$, as is plotted in Fig. 4. In fact, for this limit case when $c \to 0$

$$\sigma_{xx}(b,0) \approx \frac{2}{\pi}\int_{-b}^{b} \frac{fp_{max} sign(t)\sqrt{1-(t/b)^2}}{b-t}\,\mathrm{d}t + \sigma_b = \frac{4}{\pi} fp_{max} + \sigma_b. \tag{20}$$

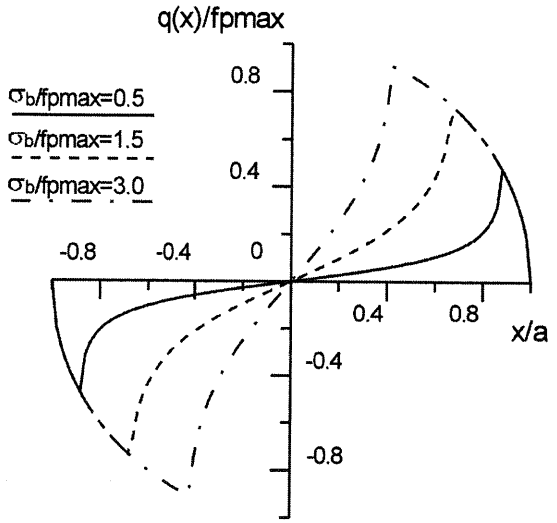

Fig. 3. Hertzian contact and bulk stress only: shear tractions $q(x)/fp_{max}$ for various levels of bulk stress σ_b/fp_{max}.

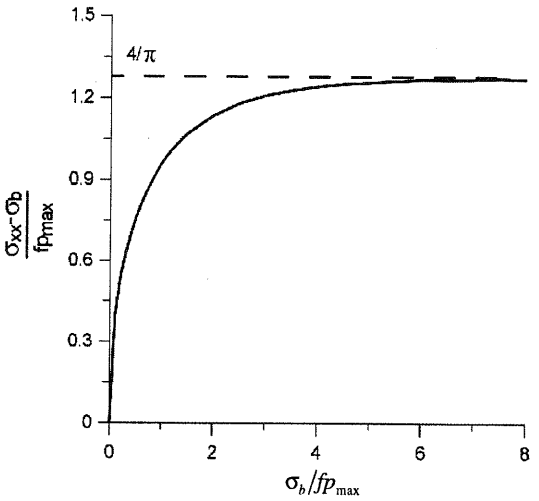

Fig. 4. Hertzian contact and bulk stress only: peak tensile stress (represented as $(\sigma_{xx} - \sigma_b)/fp_{max}$) as a function of bulk stress σ_b/fp_{max}.

2.2. Tangential load and moderate bulk stress

When both bulk tension and shear load Q are imposed, the stick zone is no longer symmetrical and so, if e is the x coordinate of centre of stick zone of width $2c$, the solution is [9]

$$q(x) = \begin{cases} f|p(x)| + q^{corr}(x), & |x-e| \leqslant c, \\ f|p(x)|, & -b \leqslant x \leqslant e-c \cup e+c \leqslant x \leqslant b, \end{cases} \tag{21}$$

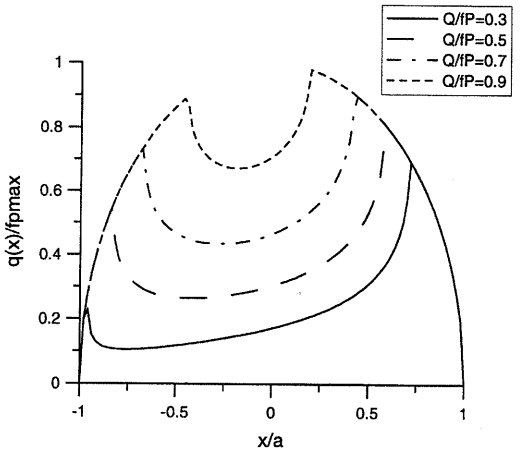

Fig. 5. Hertzian contact with tangential load and moderate bulk stress: shear tractions $q(x)/fp_{max}$ for $\sigma_b/fp_{max} = 0.5$ and various levels of Q/fP.

where

$$q^{corr}(x) = -fp_{max}\frac{c}{b}\sqrt{1-\left(\frac{(e-x)}{c}\right)^2}, \tag{22}$$

$$e/b = -\sigma_b/4fp_{max}, \quad c/b = \sqrt{1-|Q/fP|}. \tag{23}$$

It should be borne in mind that, while σ_b gives only the position of stick zone centre, the tangential force Q influences only the stick area width $2c$.

The solution holds provided that the condition $|e| + c \leqslant b$ is satisfied, or

$$\frac{\sigma_b}{4fp_{max}} + \sqrt{1-\frac{Q}{fP}} \leqslant 1 \Rightarrow \frac{\sigma_b}{fp_{max}} \leqslant 4\left(1-\sqrt{1-\frac{Q}{fP}}\right). \tag{24}$$

In the Fig. 5 the shear traction distribution is shown for several values of Q/fP and σ_b/fp_{max}=0.5. In order to evaluate the maximum tensile stress in the trailing edge we have to calculate the contributes due to the two distributions. Accordingly, there is a first therm σ_{xx}^{FS}, depending on full sliding distribution $f|p(x)|$, equal to $2fp_{max}$. Then the second contribute due to corrective traction $q^{corr}(x)$ can be found after some algebra as

$$\sigma_{xx}^{corr} = -2fp_{max}\left[1+\frac{\sigma_b}{4fp_{max}} - \sqrt{\left(1+\frac{\sigma_b}{4fp_{max}}\right)^2 - \left(1-\left|\frac{Q}{fP}\right|\right)}\right]. \tag{25}$$

In order to obtain the normal peak stress we have to sum the two contributes, due to the contact tractions, to the bulk remote load σ_b and so

$$\sigma_{xx} = \sigma_{xx}^{FS} + \sigma_{xx}^{corr} + \sigma_b = 2fp_{max}\left[\frac{\sigma_b}{4fp_{max}} + \sqrt{\left(1+\frac{\sigma_b}{4fp_{max}}\right)^2 - \left(1-\left|\frac{Q}{fP}\right|\right)}\right]. \tag{26}$$

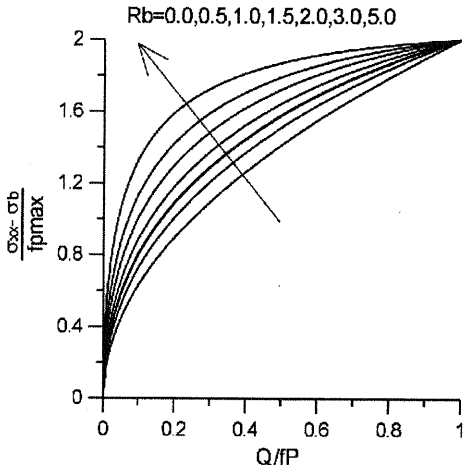

Fig. 6. Hertzian contact with tangential load and moderate bulk stress: peak tensile stress (represented as $(\sigma_{xx}-\sigma_b)/fp_{max}$) as a function of Q/fP for various levels of bulk stress $R_b < 1$.

In Fig. 6 the value of the peak as a function of the ratio Q/fP is plotted for different value of $R_b = \sigma_b/\sigma_{b,lim}$, where

$$\sigma_{b,lim} = 4fp_{max}(1 - \sqrt{1-(Q/fP)}). \tag{27}$$

If only tangential load is applied, we can find the simplified expression for the peak, that becomes

$$\sigma_{xx} = \sigma_{xx}^{FS} + \sigma_{xx}^{corr} = 2fp_{max}\sqrt{\left|\frac{Q}{fP}\right|}. \tag{28}$$

2.3. Tangential load and large bulk stress

When $\sigma_b/fp_{max} \geqslant 4(1 - \sqrt{1-Q/fP})$, the shear traction distribution assumes opposite value in sign in the two slip zones at the edges of contact. For this reason, we propose here a numerical solution, which is similar to the method first proposed by Nowell and Hills [9], with the only difference being that frictional shear tractions in the stick area $q^*(x)$, differently from Nowell and Hills [9], are taken as a product of two factors

$$q^*(r) = \phi(r)\sqrt{1-r^2} \tag{29}$$

and $\phi(r)$ is approximated by a linear combination of Chebyscheff second type polynomials

$$\phi(r) \approx \sum_{j=0}^{m} k_j U_j(r). \tag{30}$$

Fig. 7 shows the shear distribution in the case of $Q/fP = 0.5$ and $\sigma_b/fp_{max} = 2$. In the Figs. 8 and 9 the value of the stick area semiwidth and offset are plotted as a function of the ratio Q/fP for different values of $R_b = \sigma_b/\sigma_{b,lim}$ where $\sigma_{b,lim} = 4fp_{max}(1 - \sqrt{1-(Q/fP)})$. Finally, in Fig. 6 the maximum tensile stress is shown for several value of $R_b = \sigma_b/\sigma_{b\,lim} > 1$.

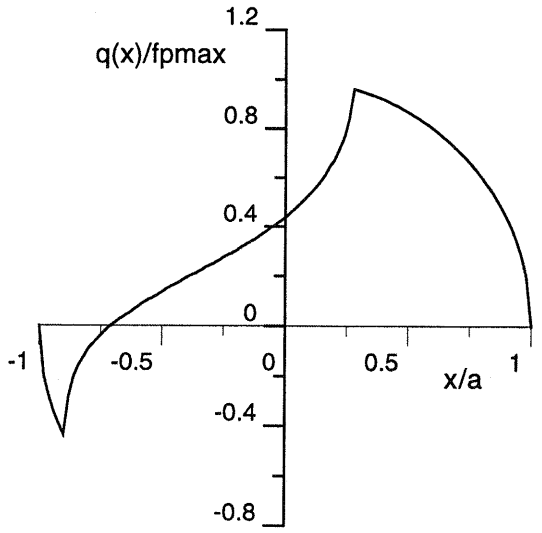

Fig. 7. Hertzian contact with tangential load and large bulk stress: shear tractions $q(x)/fp_{max}$ for $\sigma_b/fp_{max}=2$ and $Q/fP=0.5$.

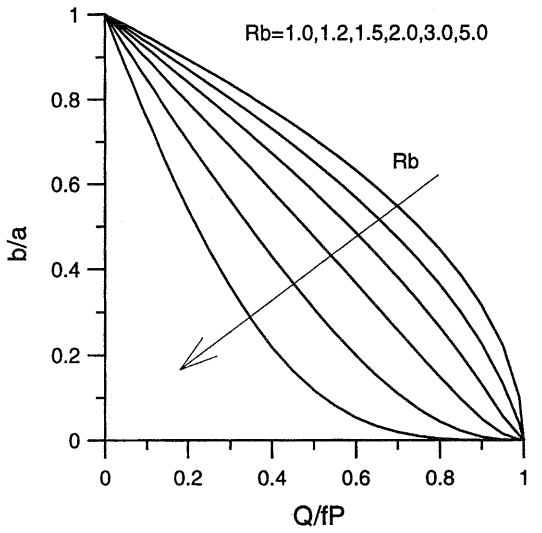

Fig. 8. Hertzian contact with tangential load and large bulk stress: variation of stick zone size b/a as a function of Q/fP for various levels of bulk stress $R_b > 1$.

3. Flat rounded punch

For dovetail joints of turbine blades, the contact problem is not strictly speaking that of a half-planes in contact. However, to reproduce a dovetail joint geometry a more realistic approximation of the geometry with respect to an Hertzian one is represented by a flat punch with rounded corners in contact with an infinite halfplane. In Fig. 10 we can see as the analogy between two

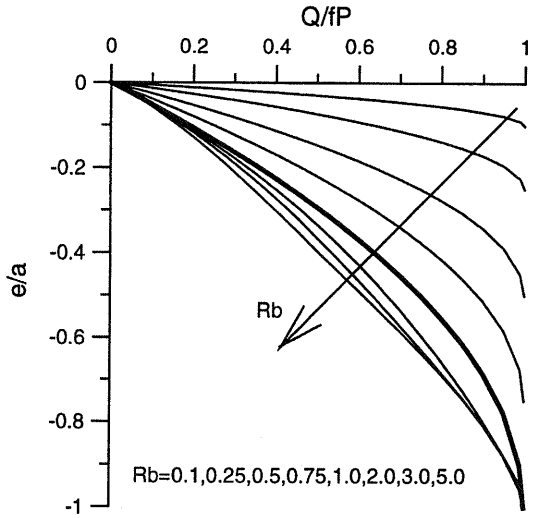

Fig. 9. Hertzian contact with tangential load and bulk stress: stick zone offset e/a as a function of Q/fP for various levels of bulk stress $R_b < 1$ (moderate bulk stress) or $R_b > 1$ (large bulk stress).

problem is well posed, because the contour gap function $h(x)$ is the same. Clearly, the loading condition on a real dovetail is much more complex than the constant normal load and oscillating tangential load plus bulk stress, but given there is a Coulomb's law limit on frictional shear, and given that the Cattaneo–Mindlin sequential case produces the highest amount of slip and accordingly of concentration of shear over the edges, we can consider this as a representative condition. The geometry shown in Fig. 10 was discussed by Ciavarella et al. [12]: the punch has a flat central part of width $2a$, and two rounded corners of radius R, approximated by parabolic curves. The pressure distribution was there given in closed form as

$$\frac{\pi^2 b}{2P}\,p(x) = \left(2\arcsin\left(\frac{a}{b}\right) - \pi\right)\frac{\sqrt{b^2-x^2}}{b} - \ln\left[\left|\frac{x\sqrt{b^2-a^2}+a\sqrt{b^2-x^2}}{x\sqrt{b^2-a^2}-a\sqrt{b^2-x^2}}\right|^{x/b}\left|\frac{\sqrt{b^2-x^2}-\sqrt{b^2-a^2}}{\sqrt{b^2-x^2}+\sqrt{b^2-a^2}}\right|^{a/b}\right]. \tag{31}$$

An alternative formulation is proposed by Jäger [13]. After fixing a certain value of parameter a, the contact area b can be evaluated using equilibrium equation:

$$\frac{PAR}{b^2} = \frac{\pi}{2} - \frac{a}{b}\sqrt{1-\left(\frac{a}{b}\right)^2} - \arcsin\left(\frac{a}{b}\right). \tag{32}$$

Fig. 11 shows the normal pressure distribution $-p(x)b/P$ for several values of ratio a/b, or from the Hertzian case for $a/b = 0$ up to the value near to completely flat punch case ($a/b \to 1$). Jäger [13] starts with the case of a flat punch with a rounded edge R on the right corner only, subjected

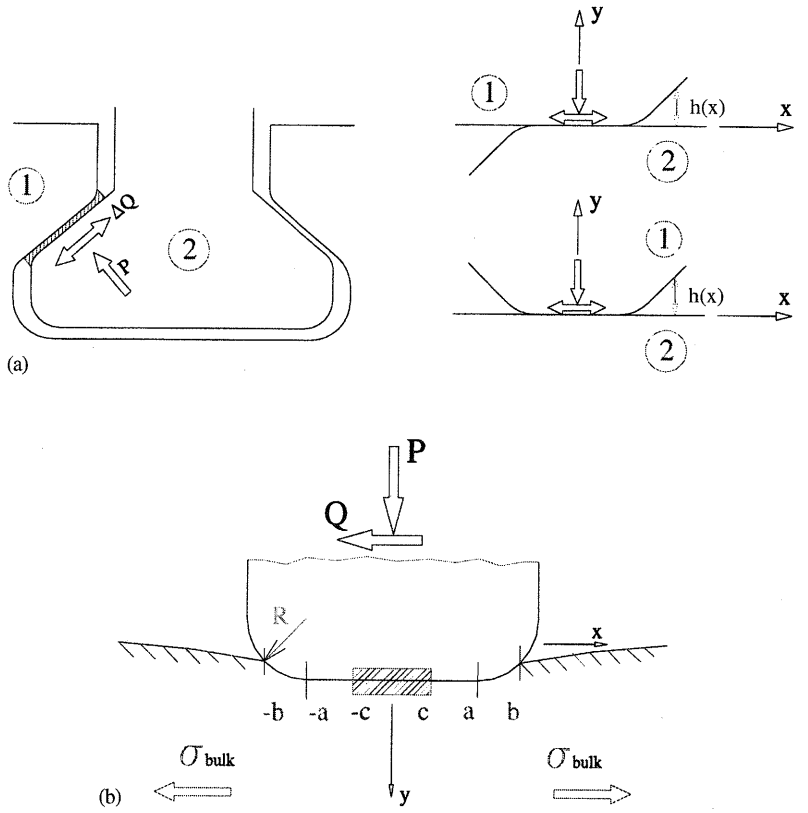

Fig. 10. Dovetail joint: (a) and flat rounded contact; (b) geometries.

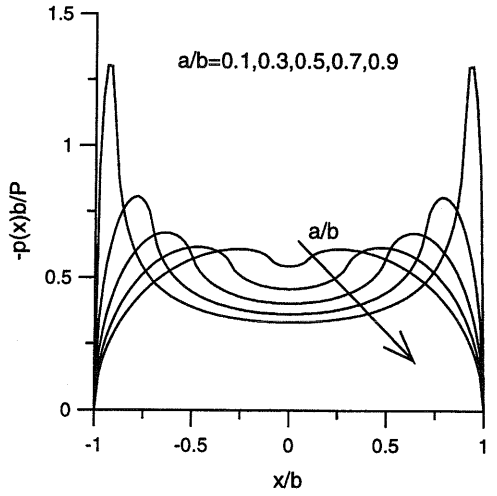

Fig. 11. Flat rounded contact pressure distribution for various geometrical ratios a/b.

to a normal load P

$$2\pi AR\phi_{p1}(z,b) = \mathrm{i}\sqrt{\frac{z-b}{z+b}}\left[(2a-2z-2b)\arccos\sqrt{\frac{a+b}{2b}} - \sqrt{b^2-a^2}\right] + 2i(z-a)\arcsin\sqrt{\frac{(z+b)(b-a)}{2b(z-a)}}, \tag{33}$$

where $z = x + \mathrm{i}y$, $\mathrm{i} = \sqrt{-1}$. The solution for a symmetric flat punch with two rounded edges can be written as symmetric superposition of two singular punches, eliminating symmetric singularities at the edges

$$\phi_p(z,b) = \phi_{p1}(z,b) + \phi_{p1}(-z,b) - \frac{\mathrm{i}b\left(\sqrt{b^2-a^2} - 2a\arccos\sqrt{\frac{a+b}{2b}}\right)}{\pi AR\sqrt{z^2-b^2}}. \tag{34}$$

The stress components can be expressed as a function of the Muskhelisvili potential

$$\sigma_{xx} + \sigma_{yy} = 2(\phi(z) + \overline{\phi(z)}), \tag{35}$$

$$\sigma_{yy} - \mathrm{i}\tau_{xy} = \phi(z) - \phi(\bar{z}) + (z-\bar{z})\overline{\phi'(z)}. \tag{36}$$

3.1. Tangential load

In the case of Cattaneo–Mindlin tangential load, the solution has been given in very general terms for any plane contact problem [10], as a superposition of

$$q(x) = f[p(x) - p^*(x)] \tag{37}$$

with $p^*(x)$ being the normal contact pressure distribution at some smaller value of the normal load. Upon increasing the tangential force, the stick zone shrinks, in the reverse order as the normal contact area during the normal loading process. The more general loading scenarios where normal load is not held constant (Mindlin problem) has also been treated in quite general terms by Jaeger [11]. Fig. 12 shows some examples for the rounded flat geometry. The Muskhelishvili potential for the tangential loading alone has been derived by Jäger [13]

$$\phi_q(z,b,c) = \mathrm{i}f(\phi_p(z,b) - \phi_p(z,c)), \tag{38}$$

where c depends on the equilibrium equation in the horizontal direction; imposing the equilibrium condition to horizontal traslation leads to the following formulation:

$$\frac{|Q|}{fP} = 1 - \left(\frac{c}{b}\right)^2 \frac{\pi/2 - (a/c)\sqrt{1-(a/c)^2} - \arcsin(a/c)}{\pi/2 - (a/b)\sqrt{1-(a/b)^2} - \arcsin(a/b)}. \tag{39}$$

Accordingly, the total potential for normal and tangential loading is

$$\phi_{tot}(z,b,c) = \phi_p(z,b) + \phi_q(z,b,c) = (1+\mathrm{i}f)\phi_p(z,b) - \mathrm{i}f\phi_p(z,c). \tag{40}$$

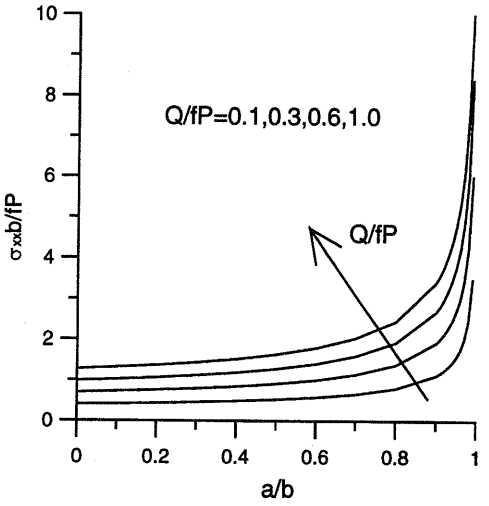

Fig. 13. Flat rounded contact and tangential load only: peak tensile stress (represented as σ_{xx}/fp_{max}) as a function of geometrical ratios a/b for various levels of Q/fP.

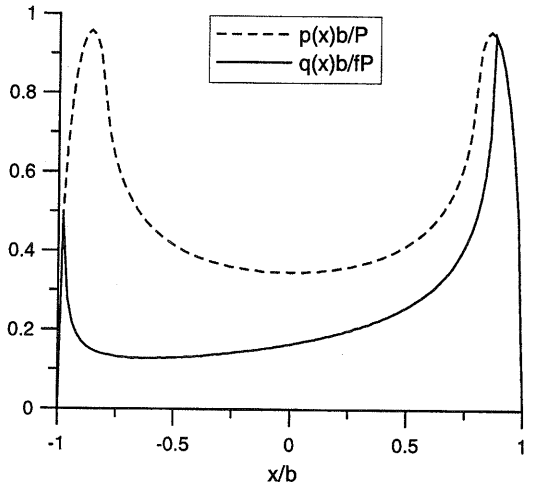

Fig. 14. Flat rounded contact with tangential load and bulk stress: shear tractions for a/b=0.8, Q/fP=0.5 and σ_b/fp_{max}=0.4.

Also in this case

$$q(x) = q^*(x), \qquad |x - e| \leqslant c,$$

$$q(x) = f|p(x)|, \quad b \leqslant x \leqslant -c + e \cup c + e \leqslant x \leqslant b, \tag{44}$$

where e indicate the x coordinate of the stick area centre respect. The same Chebyscheff polynomials method as in the case of large bulk for the Hertzian geometry is then used. Figs. 14 and 15 show two example results.

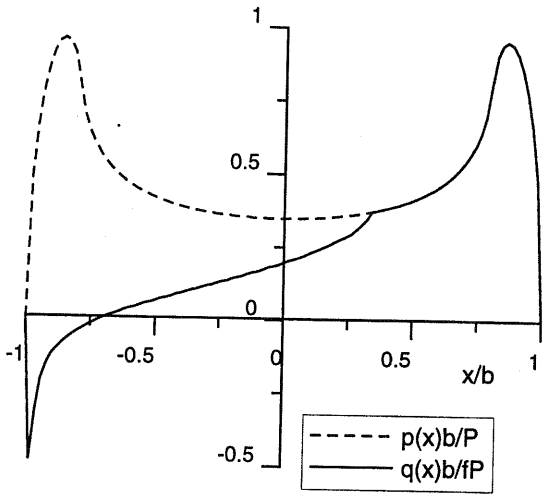

Fig. 15. Flat rounded contact with tangential load and bulk stress: shear tractions for $a/b=0.8$, $Q/fP=0.5$ and $\sigma_b/fp_{max}=1$.

Instead of presenting the full set of results for the peak at the *trailing edge* using the numerical solution, we more simply remind that an approximate equation for the peak stress has been obtained by Ciavarella et al. [16],

$$\sigma_{xx}(b,0)=2fp_{max}k\left(\sqrt{\left(1+\frac{\sigma_b}{4fp_{max}}\right)^2-\left(1-\frac{|Q|}{fP}\right)}-\frac{\sigma_{bulk}}{4fp_{max}}\right)+\sigma_b. \tag{45}$$

Notice that as usual $p_{max}=2P/\pi b=(4/\pi)p_{med}$ so it is the peak pressure only for Hertzian case. Fig. 16 shows three examples for $a/b=0.3,0.6,0.9$ as only the Hertzian case was represented in plots by Ciavarella et al. [16].

3.3. Bulk stress only

We can attempt a closed form solution in the case of flat rounded punch, by using a simplified form of the pressure distribution. The normal pressure $p(x)$ is given by Eq. (31) and can be reinterpreted as the sum of an Hertzian contribution $p_{her}(x)$, i.e. $p(x)=p_{her}(x)+p_{cor}(x)$, where the Hertzian terms is given by

$$p_{her}(x)=-k\frac{2P}{\pi b}\sqrt{1-\left(\frac{x}{b}\right)^2} \tag{46}$$

and

$$k=\sqrt{\frac{1-\frac{2}{\pi}\arcsin(a/b)}{1-\frac{2}{\pi}\arcsin(a/b)-\frac{2}{\pi}\frac{a}{b}\sqrt{1-(a/b)^2}}}. \tag{47}$$

4. Conclusions

New results have been obtained in closed form for the traction distributions and peak tensile stress of typical fretting contact problems, namely Hertz and rounded flat geometries under constant normal load and oscillating tangential and bulk loads. The most complex configurations have been solved numerically. A full description of the stress has been derived, and various effects have been considered in particular over the peak stress: the effect of the geometry from Hertzian to rounded flat indenter of various shapes up to the almost flat, and the effect of tangential and bulk stresses.

References

[1] Eden EM, Rose WN, Cunningham FL. The endurance of metals. Proceedings of the Institute of Mechanical Engineers, 875:1911.
[2] Tomlinson GA. The rusting of steel surfaces in contact. Proceedings of the Royal Society of London A 1927;115: 472–83.
[3] Nishioka K, Hirakawa K. Fundamental investigation of fretting fatigue—Part 3. Some phenomena and mechanisms of surface cracks—Part 4. The effect of mean stress—Part 5. The effect of relative slip amplitude. Bulletien of JSME 1969;12:397–407, 408–14, 692–7.
[4] Nowell D, Hills DA. Crack initiation criteria in fretting fatigue. Wear 1990;136:329–43.
[5] Ciavarella M, Demelio G. A review of analytical aspects of fretting fatigue, with extension to damage parameters, and application to dovetail joints. International Journal of Solids and Structures 2001;38(10–13):1791–811.
[6] Giannakopoulos AE, Lindley TC, Suresh S. Aspect of equivalence between contact mechanics and fracture mechanics: theoretical connections and a life-prediction methodology for fretting-fatigue. Acta Materialia 1998;46(9):2955–68.
[7] Giannakopoulos AE, Lindley TC, Suresh S. Similarities of stress concentration in contact at round punches and fatigue at notches: implication to fretting fatigue crack initiation. Fatigue and Fracture of Engineering Materials of Structures 2000;23:561–71.
[8] Cattaneo C. Sul contatto di due corpi elastici: distribuzione locale degli sforzi. Rendiconti dell'Accademia Nazionale dei Lincei 1938;27:342–8, 434–6, 474–8.
[9] Nowell D, Hills DA. Mechanics of fretting fatigue tests. International Journal of Mechanical Sciences 1987;29(5): 355–65.
[10] Ciavarella M. The generalised cattaneo partial slip plane contact problem. I-Theory. II-Examples. International Journal of Solids and Structures 1998;35/18:2349–78.
[11] Jäger J. A new principle in contact mechanics. ASME Journal of Tribology 1998;120(4):677–84.
[12] Ciavarella M, Hills DA, Monno G. The influence of rounded edges on indentation by a flat punch. IMechE Part C. Journal of Mechanical Engineering Science 1998;212(4):319–28.
[13] Jäger J. New analytical and numerical results for two-dimensional contact profiles. International Journal of Solids and Structures 2002;39(4):959–72.
[14] Hills DA, Nowell D, Sackfield A. Mechanics of elastic contacts. Oxford: Butterworth Heinemann, 1993.
[15] Spence DA. An eigenvalue problem for elastic contact with finite friction. Proceedings of the Cambridge Philosophical Society 1973;73:249–68.
[16] Ciavarella M, Macina G, Demelio GP. On stress concentration on nearly flat contacts. Journal of Strain Analysis 2002;37(6):493–501.